

Denoising and Extension of Response Functions in the Time Domain

Alexander F. Kemper,^{1,*} Chao Yang,^{2,†} and Emanuel Gull^{3,‡}

¹*Department of Physics, North Carolina State University, Raleigh, North Carolina 27695, USA*

²*Computational Research Division, Lawrence Berkeley National Laboratory, Berkeley, CA 94720, USA*

³*Department of Physics, University of Michigan, Ann Arbor, Michigan 48109, USA*

(Dated: February 1, 2024)

Response functions of quantum systems, such as electron Green’s functions, magnetic, or charge susceptibilities, describe the response of a system to an external perturbation. They are the central objects of interest in field theories and quantum computing and measured directly in experiment. Response functions are intrinsically causal. In equilibrium and steady-state systems, they correspond to a positive spectral function in the frequency domain. Since response functions define an inner product on a Hilbert space and thereby induce a positive definite function, the properties of this function can be used to reduce noise in measured data and, in equilibrium and steady state, to construct positive definite extensions for data known on finite time intervals, which are then guaranteed to correspond to positive spectra.

Introduction. Response functions are critical for the understanding of physics in a wide variety of contexts. They are a natural framework for considering *dynamical* properties that involve excitations [1–4]. Response functions are also measured in experimental setups ranging from low-frequency THz conductivity to magnetic susceptibilities and photoemission spectroscopy. A large body of literature has been devoted to the study of response functions, and a number of “field” theoretical approaches avoid the calculation of eigenstates entirely, and instead cast the formalism in terms of response functions, called correlation or Green’s functions in this context. These include embedding techniques such as the dynamical mean field theory (DMFT) [5–7] and its cluster extensions [8–11], Monte Carlo approaches for lattice [12] and impurity [13–17] models, self-consistent partial summation methods for real materials and model systems [18–20], and non-equilibrium Green’s function methods [4, 21–28].

An important characteristic of correlation functions lies in their analytical properties. The retarded correlation functions have no content at negative times due to causality [1–3]. In the complex frequency domain, they correspond to so-called Nevanlinna functions [29] whose poles are restricted to the lower half of the complex plane. This analytical framework has long been utilized to evaluate integrals that emerge in many-body theory [1–3], such as those occurring in the context of warm dense matter [30] and uniform electron liquids [31]. More recently, it was used to perform analytic continuation from a Wick-rotated frame to a standard frame. Where traditional approaches that rely e.g. on the maximum entropy method [32] have significant uncertainty in the final result, resulting in washed out spectra, explicitly enforcing the highly constraining analytical properties of Nevanlinna functions results in a drastic reduction of the uncertainty, leading to sharp spectral functions [33, 34]. It is clear from these examples that encoding this mathematical structure into numerical algorithms can be used

to great benefit.

In this Letter, we analyze a fundamental property of correlation functions in the time domain: several correlation functions of interest are *positive definite functions* of their time arguments. This property arises from viewing correlation functions as an inner product in the vector space of operators, combined with the fact that the time translation operator is a unitary representation of the time translation group. This positive definiteness sets a strong constraint on the correlation function, similar to its other analytic properties — in fact, some of these directly follow from the positive definiteness [35]. Moreover, insisting that a correlation function is positive definite enables both the extension of numerical correlation functions to later times, and the extraction of clean spectra from noisy data such as that obtained from Monte Carlo and Quantum Computing approaches.

We consider a quantum system in a quantum state ρ . In a second quantized formalism, quantum states can be described as states in Fock space [1–3]. The energetics (and dynamics) of the system is described by a Hamiltonian \mathcal{H} ; in the Heisenberg picture, the time-evolution of an operator A is given by $A(t) = e^{i\mathcal{H}t} A e^{-i\mathcal{H}t}$. Expectation values of operators for the state ρ are computed as $\langle A(t) \rangle = \text{Tr}[\rho A(t)]$. In a system with time-translational invariance, \mathcal{H} commutes with ρ , and in the canonical ensemble $\rho = e^{-\beta\mathcal{H}}/\mathcal{Z}$, with β denoting the inverse temperature and $\mathcal{Z} \equiv \text{Tr}e^{-\beta\mathcal{H}}$.

We are primarily interested in time-dependent single-particle correlation functions of the type

$$G_{AB}(t, t') = \langle A^\dagger(t) B(t') \rangle. \quad (1)$$

In a fermion system with creation operators c_i^\dagger creating particles in state i , the so-called “lesser” Green’s function [4] $G_{ij}^<(t, t') = i\text{Tr}[\rho c_j^\dagger(t') c_i(t)]$ and the “greater” Green’s function $G_{ij}^>(t, t') = -i\text{Tr}[\rho c_i(t) c_j^\dagger(t')]$, as well as the charge and spin correlation functions are related

to correlation functions of this type. Below, we consider these functions without their usual $\pm i$ prefactors.

Mathematical exposition. In this section, we will show that $G_{AB}(t, t')$ are *positive definite* functions when $A = B$. First, we observe that the correlation function can be viewed as an inner product of the linear operators that act on Fock space V (we denote this vector space as $\mathcal{L}(V)$). This fact was also noted in Ref. [36], where it was used to construct strictly positive perturbative approximations. We define an inner product on $\mathcal{L}(V)$ as

$$\langle A, B \rangle := \text{Tr} [\rho A^\dagger B], \quad (2)$$

which is conjugate symmetric, linear in the second component, and positive for $\langle A, A \rangle$ when $A \neq 0$. The properties of conjugate symmetry and linearity are straightforward to verify. The positivity property $\langle A, A \rangle \geq 0$ can be established by noting that (i) if a square matrix M equals the multiplication of a matrix with its Hermitian transpose, i.e., $M = AA^\dagger$, then M is a Hermitian positive semi-definite matrix; and (ii) the trace of the product of two positive semi-definite matrices M and N is always greater than or equal to zero, i.e., $\text{Tr}(MN) \geq 0$. We further restrict our consideration to the cases where A, B are not orthogonal to ρ , which would yield a zero expectation value and is thus not physically relevant for correlation functions. $\mathcal{L}(V)$ together with the inner product of Eq. 2 forms a Hilbert space.

The correlation functions are defined as complex-valued two-time functions ($\mathbb{R} \times \mathbb{R} \rightarrow \mathbb{C}$):

$$G_{AA}(t, t') = \text{Tr} [\rho A(t)^\dagger A(t')]. \quad (3)$$

Given the inner product, we can show that the Green's functions arising in the study of equilibrium and non-equilibrium dynamics of many-body physics [1–4] are positive definite functions [37] of two variables. That is, given any (finite) set of arbitrarily spaced time points t , the eigenvalues of the matrix that result from evaluating the Green's function at those points, $[G_{AA}(t_i, t_j)]$, are all positive or zero [38].

We prove this by using an equivalent definition of positive definiteness, which is that, given the aforementioned set of time points t ,

$$\sum_{ij} G_{AA}(t_i, t_j) \lambda_i^* \lambda_j \geq 0 \quad (4)$$

for any set of λ_i . This follows from

$$\begin{aligned} \sum_{ij} G_{AA}(t_i, t_j) \lambda_i^* \lambda_j &= \sum_{i,j} \text{Tr} [\rho A(t_i)^\dagger A(t_j)] \lambda_i^* \lambda_j \\ &= \text{Tr} \left[\rho \left(\sum_i \lambda_i A(t_i) \right)^\dagger \left(\sum_j \lambda_j A(t_j) \right) \right] \\ &= \left\langle \sum_i \lambda_i A(t_i), \sum_j \lambda_j A(t_j) \right\rangle \geq 0. \end{aligned} \quad (5)$$

The correlation functions (and Green's function as well as self-energies [39, 40]) are therefore positive definite functions. This holds for any operator $A \in \mathcal{L}(V)$, and in particular it holds for fermionic creation/annihilation operators c^\dagger/c , for densities n , for magnetization operators $n_\uparrow - n_\downarrow$, and trivially for the identity. In multi-orbital systems, the diagonal components of electronic Green's functions G_{ii}^{\lessgtr} are positive semi-definite. Off-diagonal components can be constructed from linear combinations of $\langle c_i + c_j, c_i + c_j \rangle$, $\langle c_i + ic_j, c_i + ic_j \rangle$, and the diagonal components, all of which are positive definite.

In the presence of time-translation invariance, (*i.e.* for steady-state and equilibrium systems), the Green's function becomes a function of a single time argument corresponding to the time difference: $G_{AA}(t - t')$, *i.e.* a positive definite function of a single variable where

$$\sum_{ij} G_{AA}(t_i - t_j) \lambda_i^* \lambda_j \geq 0. \quad (6)$$

In order for time translation to hold, the set of time points t must form a group under addition such as \mathbb{R} or \mathbb{Z} . With this additional structure, and as long as ρ commutes with the time evolution operator,

$$\langle A(t), B(t') \rangle = \langle A(t - t'), B \rangle = \langle A, B(t' - t) \rangle \quad (7)$$

follows from the cyclicity of the trace. Additional mathematical details are provided in the supplement.

The positive definiteness of the Green's function sets a strong constraint on the function and has important practical consequences, which we will explore and exploit in the remainder of the paper. In short, we will show that (i) we can improve the signal-to-noise ratio in noisy data from experiment and theory, and (ii) we can construct causal extensions (with a positive spectrum) from short time data.

Denosing correlation functions. A first, and natural application of the mathematics presented above, is to take a correlation function from a source that has some inherent noise, and to use the positive definite property to project its values to the nearest positive definite correlation function; in effect, denosing the data. Noisy correlation functions can arise from Monte Carlo evaluations, from experimental measurements, or from simulations on quantum computers.

We consider a discretized, time-translation invariant correlation function on a regularly spaced time axis t , $G_{AA}(t_i - t_j)$. If we label the elements of the correlation function as $G_{AA}(t_i - t_j) \rightarrow f_{i-j}$, then the resulting matrix \underline{G} with entries $\underline{G}_{ij} = f_{i-j}$ is a positive semi-definite Hermitian Toeplitz matrix [37],

$$\underline{G} = \begin{pmatrix} f_0 & f_1 & f_2 & \cdots & f_n \\ f_1^* & f_0 & f_1 & \cdots & f_{n-1} \\ f_2^* & f_1^* & f_0 & \cdots & f_{n-2} \\ \vdots & & & \ddots & \vdots \\ f_n^* & f_{n-1}^* & f_{n-2}^* & \cdots & f_0 \end{pmatrix}. \quad (8)$$

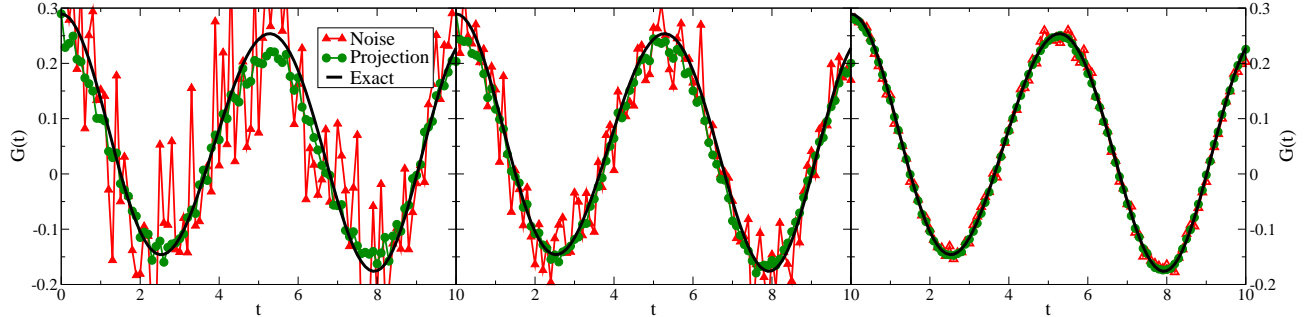


FIG. 1. Real part of the on-site Hubbard dimer Green's function $G_{11\uparrow}^>(t)$. Red triangles: Data polluted by Gaussian noise with $\sigma = 0.1$ (left panel), $\sigma = 0.05$ (middle), and $\sigma = 0.01$ (right). Green filled circles: Projection to nearest causal function. Black circles: Exact solution. Other parameters are: temperature $T = 1/10$, hopping $t = 1$, interaction $U = 5$, level energy $\epsilon = 2.3$.

\underline{G} is commonly known as the Gramian or ‘‘Gram’’ matrix.

In the presence of noise in the correlation function data (f_j), this matrix is not positive semi-definite (PSD). However, an alternating projection to the nearest PSD matrix [41] followed by projections to the nearest Toeplitz matrix [42] and an enforcement of the value at time zero (which is typically known precisely, *e.g.* from equal-time measurements or sum rules) results in quick convergence to a positive definite function.

The projection to the nearest PSD matrix is achieved by diagonalizing G and setting all negative eigenvalues to zero. The projection to the nearest Toeplitz matrix averages entries diagonally, and the enforcement of the norm consists of fixing the diagonal to a predetermined value. While an alternating projection typically converges in less than 100 iterations, faster converging schemes, see *e.g.* [43, 44] and [45], may be substantially more efficient; we have not explored them here.

We illustrate the denoising in Fig. 1 for a positive definite Green's function of the Hubbard dimer which has been polluted with Gaussian noise. Enforcing positive definiteness by the procedure above shows a dramatic improvement of the quality of the data. Details and a second application to state-of-the-art quantum Monte Carlo data with a continuous spectrum [28] are presented in the supplement.

Extending correlation functions to longer times. A second consequence of positive definiteness is that positive definite extensions of response functions to longer times exist, from which spectral measures can be constructed. We make use of two well-known mathematical facts for positive definite functions. First, functions that are only known on a subset of their domain (*e.g.* \mathbb{Z} or \mathbb{R}) have at least one extension to the full domain [46–48]. This is a consequence of the extension theorems of Kreĭn (in the case of \mathbb{R}) and Carathéodory (in the case of \mathbb{Z}). Second, according to Bochner's theorem [35], the Fourier transform of a positive definite function (over \mathbb{Z} or \mathbb{R}) is guaranteed to have positive real part; moreover, the inverse Fourier transform of a positive spectral function is

guaranteed to be positive definite. In the discrete case, these extensions may not be unique; in the continuum case, uniqueness is guaranteed by the analyticity of the Green's function.

Conceptually, this realization offers a straightforward methodology to obtain causal spectral functions from finite-time data: in a first step, the function is extended from short to long times by taking advantage of an extension theorem. In a second step, the uniquely defined and positive Fourier transform of the extended data is computed.

Numerically, we can use extension theorems to predict Green's function values at later times from known values at short times [37]. Supplementing a known time series f_0, \dots, f_n by a single unknown element f_{n+1} , the Gramian of Eq. 8 is a Toeplitz matrix with a single unknown complex number $f_{n+1} = \underline{G}_{0,n+1} = (\underline{G}_{n+1,0})^*$. The real and imaginary parts of f_{n+1} can then be obtained in a two-dimensional search in the complex plane for the region where the lowest eigenvalue of G is zero or larger, *i.e.* G is positive definite; such a value must exist [46] and $|f_{n+1}| \leq f_0$ due to the positive definiteness [49]. In practice, we find that in systems with only few well-defined excitations, and consequentially a low-rank Gram matrix, the search converges quickly to a unique solution, whereas systems with continuous spectra may present ambiguities in the extensions. Fig. 2 demonstrates the approach for the Green's function of the Hubbard dimer (for details see supplement). Once the data is extended to all times, it yields a unique spectral function [35].

More generally, given that the Gram matrix Eq. 8 is a Toeplitz matrix of size n , and assuming a rank of size r , a classical result by Carathéodory and Fejér [50] guarantees the existence of the decomposition $T = APA^\dagger$, where A is a $n \times r$ Vandermonde matrix and P is a $r \times r$ positive diagonal matrix. The columns of A can be interpreted as uniformly sampled oscillation frequencies, and the entries of P as positive ‘pole strengths’. This approach therefore gives both access to the spectral function in terms of a series of r discrete poles at given

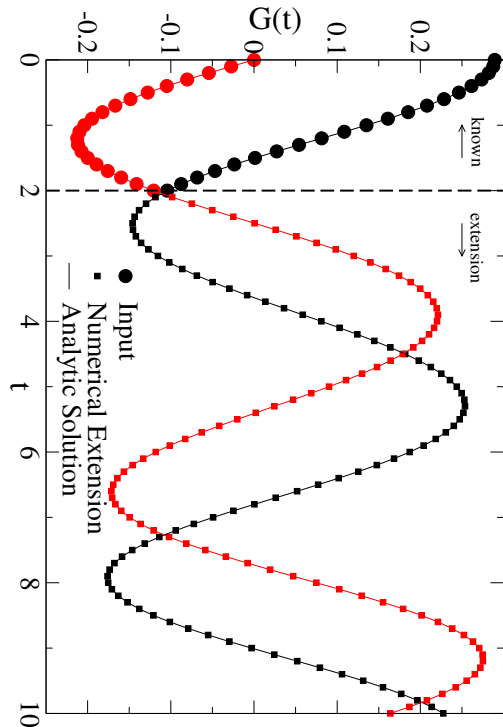


FIG. 2. Extension of the on-site Hubbard dimer Green's function $G_{11\uparrow}^>(t)$. Shown are real (black) and imaginary (red) parts of input data up to $t = 2$ (circles), the numerically computed extension from $t = 2$ to $t = 10$ (squares), and the analytically known Green's function up to $t = 10$ (lines).

frequencies, and a method to construct extensions for all times by enlarging the matrix A with additional frequencies. The decomposition also establishes a connection to signal processing and control theory, where PSD covariance matrices of time-invariant processes are analyzed using this decomposition in super-resolution algorithms such as the multiple signal classification (MUSIC) [51], and where thereby approximate extensions from noisy data can be constructed. We will explore this connection, together with connections to reproducing kernel Hilbert spaces [52], in a future paper.

Application to Quantum Computing. As a final illustration, we apply the denoising and extension implications of Eq. 6 to a noisy correlation function measured on IBM's quantum computer *ibm_auckland*. We have measured the momentum-space greater Green's function for the empty state $G_k(t) := \langle 0 | c_k^\dagger(t) c_k | 0 \rangle$ for an 8-site Su-Schrieffer-Heeger model, which is a model for free electrons with a hopping parameter that alternates with an amplitude δ

$$\mathcal{H} = -V_{nm} \sum_i [1 + (-\delta)^i] c_i^\dagger c_{i+1} + \text{H.c.} - \mu \sum_i c_i^\dagger c_i, \quad (9)$$

where we set $V_{nm} = 1$. The raw data (originally published in Ref. 53), is shown in Fig. 3, in the gapped phase with $\delta = 0.4$ at $k = \pi/2$. We report details of the calculation in the Supplementary information. Because the model is translationally invariant and has 2 bands, the momentum basis Green's functions should exhibit at most 2 frequencies. However, due to the hardware noise from the quantum computer, there is significant noise in the time domain signal. This is similarly reflected in the Fourier transform, where peaks can be identified, but only in the power spectrum — the spectral function (shown in Fig. 3) does not show the requisite analytic structure (a consistent sign across all frequencies). We de-noise the data by asserting the positive definiteness and performing a point-by-point optimization on the Green's function, where the cost function is the square of the negative eigenvalues, and obtain an improved spectrum. As can be seen in the Figure, much of the broad spectrum noise has disappeared and the peaks are clearly visible in the spectral function. We detail the procedure and show the result on additional data from different k points in the supplement; we find that this iterative procedure is more suitable in the presence of extreme noise than the alternating projection scheme used for Monte Carlo data. The final step is to extend the data as discussed above, which results in a long positive definite signal, with sharp peaks in the spectrum.

Note that applying a PSD projection as done here is conceptually distinct from recent efforts using advanced signals processing approaches to extract a cleaner signal from noisy quantum simulation [54–56], and in fact can be used as a complementary tool.

Discussion. Positive semidefinite response functions are ubiquitous in many-body physics [1, 4, 57], as is the desire to reduce systematic or stochastic noise and to obtain corresponding spectral functions. The theory and algorithms presented here are broadly applicable to problems ranging from the analysis of experimental measurements to simulations of quantum systems on classical and quantum hardware.

In this Letter, we have demonstrated the efficiency of removing noise with a PSD projection in the examples of synthetic data and real-world quantum computing data, as well as the feasibility of extending data to long time. We believe that a PSD noise filter followed by an extension should be applied much more broadly to any positive definite response function, simulated or measured, before data is analyzed and/or spectra are computed, including data from quantum Monte Carlo, tensor networks, and time-resolved experiment.

While the examples in this work focused on Green's functions, a PSD projection is not limited to this particular use case since the operators in Eq. 4 are general. For example, the identity operator is included, and thus quantities of the form $\langle \psi_0 | e^{-i\mathcal{H}t} | \psi_0 \rangle$ are also amenable to denoising in the same way. This covers a range of

novel quantum algorithms that make use of such quantities, including subspace expansions [58, 59] and energy minimization based on quantum phase estimation [60], as well as Loschmidt echo measurements [61].

We note that, similar to the extension techniques presented in this letter, memory kernel approaches [62–67] pioneered in transport physics aim to extend data measured for short times to longer times. The approach presented is complementary to those techniques and may be combined with them.

The connection highlighted here between positive definite response functions and the Toeplitz Vandermonde decomposition of the Gram matrix in addition allows to make a connection to algorithms developed for signal processing and control theory, such as MUSIC [51], which are used to analyze positive semidefinite covariance matrices. This analysis will be the topic of a future paper.

We thank Vadym Adamyan for making us aware of extension theorems, Zoltan Sasvári for pointing out the possibility of considering a Gram matrix extended by a single point, Efehan Kökcü for suggestions regarding non-equilibrium Green’s functions, and Michael Ragone for feedback on the mathematical exposition. AFK was supported by the Department of Energy, Office of Basic Energy Sciences, Division of Materials Sciences and En-

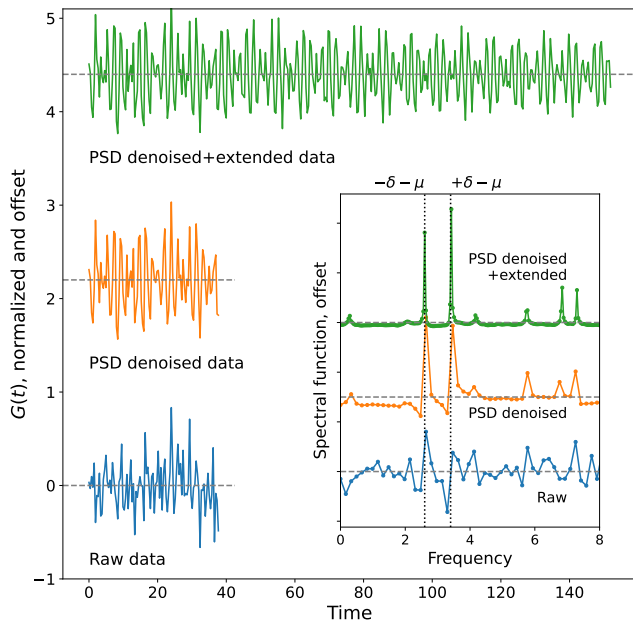


FIG. 3. Main panel: greater Green’s function $G_k^>(t)$ at $k = \pi/2$ of an 8-site Su-Schrieffer-Heeger with $\delta = 0.4$ and $\mu = -3$. The figure shows the raw data obtained from the *ibm_auckland* quantum computer (blue), as well as the PSD denoised data (orange), and PSD denoised and extended data (green). Inset: Corresponding spectral functions. The Fourier transform used a damping factor $\tau = 100$. The vertical dashed lines indicate the expected analytic frequencies.

gineering under grant no. DE-SC0023231. EG and CY were supported by the U.S. Department of Energy, Office of Science, Office of Advanced Scientific Computing Research and Office of Basic Energy Science, Scientific Discovery through Advanced Computing (SciDAC) program under Award Number(s) DE-SC0022088. The data for the figures are submitted as a supplement to this paper.

* akemper@ncsu.edu

† cyang@lbl.gov

‡ egull@umich.edu

- [1] A. Abrikosov, L. Gorkov, I. Dzyaloshinski, and R. Silverman, *Methods of Quantum Field Theory in Statistical Physics*, Dover Books on Physics (Dover Publications, 2012).
- [2] G. D. Mahan, *Many Particle Physics* (Springer, New York, NY10013, USA, 2010).
- [3] H. Bruus and K. Flensberg, *Many-body quantum theory in condensed matter physics: an introduction* (OUP Oxford, 2004).
- [4] G. Stefanucci and R. van Leeuwen, *Nonequilibrium Many-Body Theory of Quantum Systems: A Modern Introduction*, 1st ed. (Cambridge University Press, 2013).
- [5] W. Metzner and D. Vollhardt, *Phys. Rev. Lett.* **62**, 324 (1989).
- [6] A. Georges and G. Kotliar, *Phys. Rev. B* **45**, 6479 (1992).
- [7] A. Georges, G. Kotliar, W. Krauth, and M. J. Rozenberg, *Reviews of Modern Physics* **68**, 13 (1996).
- [8] M. H. Hettler, A. N. Tahvildar-Zadeh, M. Jarrell, T. Pruschke, and H. R. Krishnamurthy, *Phys. Rev. B* **58**, R7475 (1998).
- [9] A. I. Lichtenstein and M. I. Katsnelson, *Phys. Rev. B* **62**, R9283 (2000).
- [10] G. Kotliar, S. Y. Savrasov, G. Pálsson, and G. Biroli, *Phys. Rev. Lett.* **87**, 186401 (2001).
- [11] T. Maier, M. Jarrell, T. Pruschke, and M. H. Hettler, *Reviews of Modern Physics* **77**, 1027 (2005).
- [12] R. Blankenbecler, D. J. Scalapino, and R. L. Sugar, *Phys. Rev. D* **24**, 2278 (1981).
- [13] J. E. Hirsch and R. M. Fye, *Phys. Rev. Lett.* **56**, 2521 (1986).
- [14] A. N. Rubtsov, V. V. Savkin, and A. I. Lichtenstein, *Phys. Rev. B* **72**, 035122 (2005).
- [15] P. Werner, A. Comanac, L. de’ Medici, M. Troyer, and A. J. Millis, *Phys. Rev. Lett.* **97**, 076405 (2006).
- [16] E. Gull, P. Werner, O. Parcollet, and M. Troyer, *Europhysics Letters* **82**, 57003 (2008).
- [17] E. Gull, A. J. Millis, A. I. Lichtenstein, A. N. Rubtsov, M. Troyer, and P. Werner, *Rev. Mod. Phys.* **83**, 349 (2011).
- [18] L. Hedin, *Phys. Rev.* **139**, A796 (1965).
- [19] N. E. Bickers, D. J. Scalapino, and S. R. White, *Phys. Rev. Lett.* **62**, 961 (1989).
- [20] C.-N. Yeh, S. Isakov, D. Zgid, and E. Gull, *Phys. Rev. B* **106**, 235104 (2022).
- [21] L. Mühlbacher and E. Rabani, *Phys. Rev. Lett.* **100**, 176403 (2008).
- [22] P. Werner, T. Oka, and A. J. Millis, *Phys. Rev. B* **79**,

- 035320 (2009).
- [23] E. Gull, D. R. Reichman, and A. J. Millis, *Phys. Rev. B* **84**, 085134 (2011).
- [24] H. Aoki, N. Tsuji, M. Eckstein, M. Kollar, T. Oka, and P. Werner, *Rev. Mod. Phys.* **86**, 779 (2014).
- [25] M. Schüler, D. Golež, Y. Murakami, N. Bittner, A. Herrmann, H. U. Strand, P. Werner, and M. Eckstein, *Computer Physics Communications* **257**, 107484 (2020).
- [26] X. Dong, E. Gull, and H. U. R. Strand, *Phys. Rev. B* **106**, 125153 (2022).
- [27] Y. Núñez Fernández, M. Jeannin, P. T. Dumitrescu, T. Kloss, J. Kaye, O. Parcollet, and X. Waintal, *Phys. Rev. X* **12**, 041018 (2022).
- [28] A. Erpenbeck, E. Gull, and G. Cohen, *Phys. Rev. Lett.* **130**, 186301 (2023).
- [29] V. Adamyan, Y. Berezansky, I. Gohberg, M. Gorbachuk, V. Gorbachuk, A. Kochubei, H. Langer, and G. Popov, *Modern Analysis and Applications: The Mark Krein Centenary Conference - Volume 1: Operator Theory and Related Topics*, Operator Theory: Advances and Applications (Birkhäuser Basel, 2009).
- [30] J. Vorberger, Z. Donko, I. M. Tkachenko, and D. O. Gericke, *Phys. Rev. Lett.* **109**, 225001 (2012).
- [31] A. V. Filinov, J. Ara, and I. M. Tkachenko, *Phys. Rev. B* **107**, 195143 (2023).
- [32] M. Jarrell and J. Gubernatis, *Physics Reports* **269**, 133 (1996).
- [33] J. Fei, C.-N. Yeh, and E. Gull, *Physical Review Letters* **126**, 056402 (2021).
- [34] J. Fei, C.-N. Yeh, D. Zgid, and E. Gull, *Phys. Rev. B* **104**, 165111 (2021).
- [35] S. Bochner, *Vorlesungen über Fouriersche Integrale* (Leipzig : Akademische Verlagsgesellschaft, 1932).
- [36] M. J. Hyrkäs, D. Karlsson, and R. van Leeuwen, *Journal of Physics A: Mathematical and Theoretical* **55**, 335301 (2022).
- [37] Z. Sasvári, *Positive Definite and Definitizable Functions* (Berlin: Akademie Verlag, 1994).
- [38] Note that in the standard terminology that positive definite functions include zero eigenvalues [37].
- [39] K. Balzer and M. Eckstein, *Phys. Rev. B* **89**, 035148 (2014).
- [40] C. Gramsch and M. Potthoff, *Phys. Rev. B* **92**, 235135 (2015).
- [41] N. J. Higham, *Linear Algebra and its Applications* **103**, 103 (1988).
- [42] M. G. Eberle and M. C. Maciel, *Computational & Applied Mathematics* **22**, 1–18 (2003).
- [43] H. H. Bauschke and J. M. Borwein, *SIAM Review* **38**, 367 (1996), <https://doi.org/10.1137/S0036144593251710>.
- [44] H. H. Bauschke, P. L. Combettes, and D. R. Luke, *Journal of the Optical Society of America. A, Optics, image science, and vision* **19** **7**, 1334 (2002).
- [45] A. S. Lewis, D. R. Luke, and J. Malick, *Foundations of Computational Mathematics* **9**, 485 (2009).
- [46] C. Carathéodory, *Mathematische Annalen* **64**, 95 (1907).
- [47] M. Krein, in *Comptes Rendus de l'Académie des Sciences de l'URSS*, Vol. 46 (1940) pp. 17–22.
- [48] Z. Sasvári, The extension problem for positive definite functions. a short historical survey, in *Operator Theory and Indefinite Inner Product Spaces: Presented on the occasion of the retirement of Heinz Langer in the Colloquium on Operator Theory, Vienna, March 2004*, edited by M. Langer, A. Luger, and H. Woracek (Birkhäuser Basel, Basel, 2006) pp. 365–379.
- [49] We thank Z. Sasvári for suggesting this approach.
- [50] C. Caratheodory and L. Fejér, *Rendiconti del Circolo Matematico di Palermo (1884-1940)* **32**, 218 (1911).
- [51] R. Schmidt, *IEEE Transactions on Antennas and Propagation* **34**, 276 (1986).
- [52] V. I. Paulsen and M. Raghupathi, *An Introduction to the Theory of Reproducing Kernel Hilbert Spaces*, Cambridge Studies in Advanced Mathematics (Cambridge University Press, 2016).
- [53] E. Kökcü, H. A. Labib, J. Freericks, and A. F. Kemper, arXiv preprint arXiv:2302.10219 (2023).
- [54] D. Cruz and D. Magano, arXiv preprint arXiv:2210.04919 (2022).
- [55] T. Steckmann, T. Keen, E. Kökcü, A. F. Kemper, E. F. Dumitrescu, and Y. Wang, *Physical Review Research* **5**, 023198 (2023).
- [56] Y. Shen, D. Camps, S. Darbha, A. Szasz, K. Klymko, N. M. Tubman, R. Van Beeumen, *et al.*, arXiv preprint arXiv:2306.01858 (2023).
- [57] G. S. Uhrig, M. H. Kalthoff, and J. K. Freericks, *Physical Review Letters* **122**, 130604 (2019).
- [58] C. L. Cortes, A. E. DePrince III, and S. K. Gray, *Physical Review A* **106**, 042409 (2022).
- [59] K. Klymko, C. Mejuto-Zaera, S. J. Cotton, F. Wudarski, M. Urbanek, D. Hait, M. Head-Gordon, K. B. Whaley, J. Moussa, N. Wiebe, *et al.*, *PRX Quantum* **3**, 020323 (2022).
- [60] Z. Ding and L. Lin, *PRX Quantum* **4**, 020331 (2023); arXiv preprint arXiv:2303.05714 (2023).
- [61] A. Schuckert, A. Bohrdt, E. Crane, and M. Knap, arXiv preprint arXiv:2206.01756 (2022).
- [62] Q. Shi and E. Geva, *The Journal of Chemical Physics* **119**, 12063 (2003), https://pubs.aip.org/aip/jcp/article-pdf/119/23/12063/10853520/12063_1_online.pdf.
- [63] G. Cohen and E. Rabani, *Phys. Rev. B* **84**, 075150 (2011).
- [64] G. Cohen, E. Gull, D. R. Reichman, A. J. Millis, and E. Rabani, *Phys. Rev. B* **87**, 195108 (2013).
- [65] J. Cerrillo and J. Cao, *Phys. Rev. Lett.* **112**, 110401 (2014).
- [66] F. A. Pollock and K. Modi, *Quantum* **2**, 76 (2018).
- [67] F. A. Pollock, E. Gull, K. Modi, and G. Cohen, *SciPost Phys.* **13**, 027 (2022).
- [68] G. Cohen, E. Gull, D. R. Reichman, and A. J. Millis, *Phys. Rev. Lett.* **115**, 266802 (2015).

Application to quantum computer data

Fig. S1 shows the greater Green's function obtained from IBM quantum computers for the Su-Schrieffer-Heeger (SSH) model

$$\mathcal{H} = - \sum_{\langle i,j \rangle} [V_{nn} + (-1)^i \delta/2] c_i^\dagger c_j - \mu \sum_i c_i^\dagger c_i. \quad (10)$$

This data was originally presented in Kökcü et al. [53]. The figure shows the data for $\delta = 0.4$, $\mu = -3$, and momenta $k \in \{0, 1, 2, 3, 4\} \frac{2\pi}{8}$. Note that while the Fourier transform power spectrum shows peaks near the expected values (indicated as vertical dashed lines), there is a substantial amount of noise present.

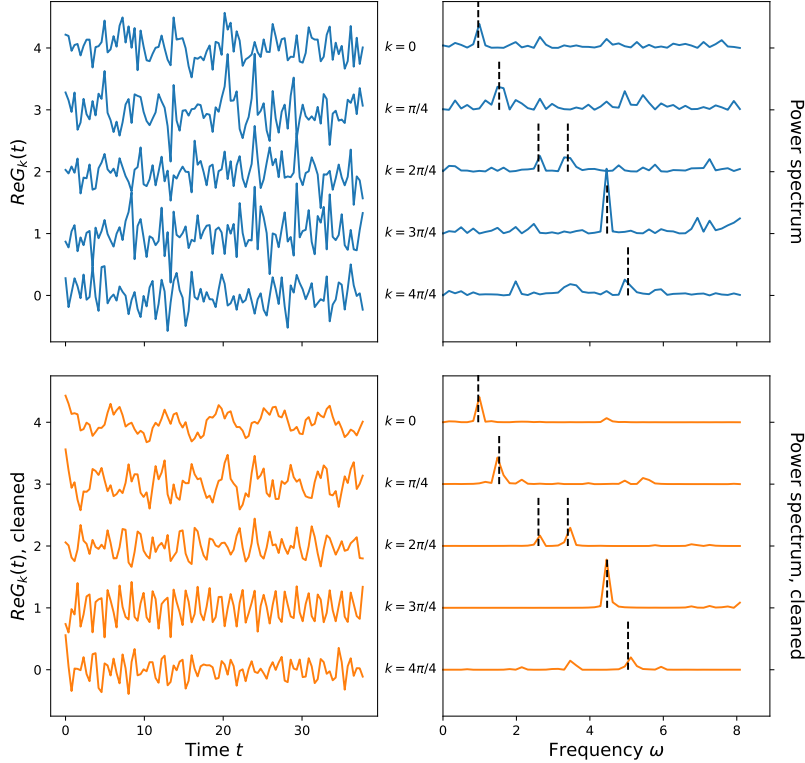


FIG. S1. Top panel: Raw data for an 8-site Green's function $\text{Re}G_k(t)$ and corresponding power spectrum for the SSH model with $\delta = 0.4$ and $\mu = -3$ obtained from IBM's quantum computer *ibm_auckland* (originally from Ref. [53]). Bottom panel: Data after PSD denoising as discussed below. Individual curves are k points. The dashed lines indicate the expected frequencies obtained by analytically solving Eq. 10.

The Gramian of the Green's function, *i.e.* the Toeplitz matrix constructed from the Green's function, must follow the structure of Eq. (8) and be positive semidefinite. In the presence of noise, the Gramian is a Toeplitz matrix but is not positive definite. Defining a cost function

$$\mathcal{C} = \sum_i [\lambda_i (\text{sgn}(\lambda_i) - 1)]^2 \quad (11)$$

where λ_i are the eigenvalues of G , we cycle through the individual entries in G and numerically optimize them with respect to this cost function. In cases with very large noise, such as with data from quantum computers, we find this procedure to be more reliable than the alternating projection described in the main text.

We apply this approach to the data set from Ref. [53] with the worst quality, $\delta = 0.4$; the results are shown in Fig. S1. For most of the momenta, the assertion that the Green's function should have the structure of Eq. (8) yield quite good results — the algorithm correctly picks out the correct peak(s) in the Fourier transform. The notable exception is the $k = \pi$, which is because the original data is particularly poor.

Application to steady-state Monte Carlo data

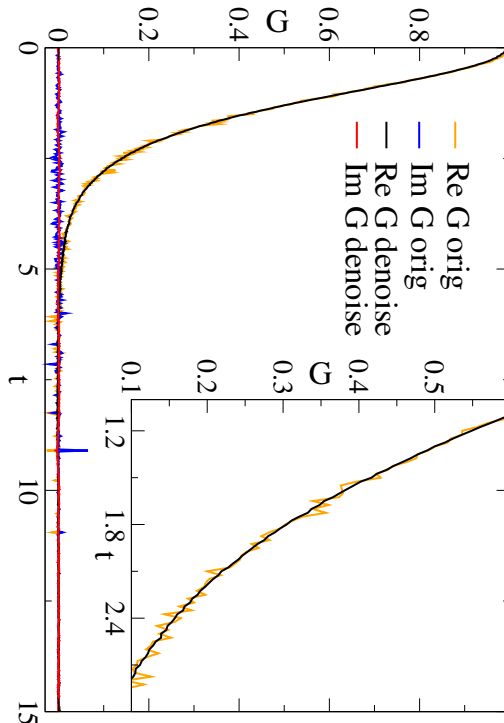


FIG. S2. De-noised Quantum Monte Carlo data. Main panel: inchworm [68] quantum Monte Carlo of a steady-state transport problem (for data and parameters see Fig. 1 of [28]), real part (orange) and imaginary part (blue). Denoised data, real part (black) and imaginary part (red). Inset: Zoom into the region near $t=2$ highlighting the effect of denoising.

In this section, we present de-noised data from a real-time simulation with current state-of-the-art quantum Monte Carlo technology. We use the steady-state formulation [28] of the Inchworm [68] Monte Carlo real-time propagation scheme. The method overcomes the dynamical sign problem inherent to many real-time Monte Carlo methods [17, 21] and is therefore able to simulate transport data for long times.

The data presented has Monte Carlo noise whose size differs as a function of time but is largest in the region near $t = 2$. Visible are also data ‘glitches’ near $t = 9.1$ which are likely due to ergodicity issues in the simulation and which are clearly unphysical.

We employ the alternate projection described in the main text, while keeping the norm fixed to the known analytical value of 1. It is evident that the causal projection onto a positive definite function eliminates much of the Monte Carlo noise and results in a real-time function that is much smoother. Unphysical outliers in the data are eliminated. Obtaining data of the same quality as the de-noised data would require a substantially larger investment of computer time.

The Hubbard Dimer – Details

For the data in Fig. 1, we consider a Hubbard dimer (a two-site Hubbard model) with the following Hamiltonian:

$$H = H_0 + H_I, \quad (12)$$

$$H_0 = -\epsilon \sum_{i=1,2} (n_{i\uparrow} + n_{i\downarrow}) - v \sum_{\sigma=\uparrow,\downarrow} c_{0\sigma}^\dagger c_{1\sigma} + c_{1\sigma}^\dagger c_{0\sigma}, \quad (13)$$

$$H_I = U \sum_{i=1,2} \left(n_{i\uparrow} n_{i\downarrow} - \frac{1}{2} (n_{i\uparrow} + n_{i\downarrow}) \right) \quad (14)$$

The operators $c_{i\sigma}$ describe four fermion annihilation operators that annihilate particles on site $i = 1, 2$ with spin $\sigma = \uparrow, \downarrow$. Their adjoints $c_{i\sigma}^\dagger$ create the corresponding particles on site i with spin σ . These operators correspond to matrices of size 16×16 in Fock space and satisfy the fermion commutation rules.

The parameter U describes the on-site repulsion and is set to $U = 5$. ϵ is an on-site level energy term ($\epsilon = 0$ corresponds to half filling), and v describes the hopping between sites 1 and 2. At temperature $T = 1/\beta = 0.1$, the choice of $\epsilon = 2.3$ corresponds to a density of 0.710556 on all spin-orbitals.

The Green's function discussed in Fig. 1 is defined as

$$G_{11\uparrow}(t) = \frac{1}{Z} \text{Tr} \left[e^{(-\beta+it)H} c_{1\uparrow} e^{-itH} c_{1\uparrow}^\dagger \right], \quad (15)$$

and is a positive definite function that is symmetric in the real part and anti-symmetric in the imaginary part, with $G_{11\uparrow}(t=0) = 0.289444$. (note that the system is degenerate in site and spin indices). The positive definite function corresponds, up to a factor of $-i$, to the spin-up on-site greater Green's function of site 1 of the system.

Additional Mathematical notes

In an attempt to make the presentation in the main text accessible to most physicists, we have eliminated some of the more formal mathematical aspects. We would like to highlight the following additional connections:

Inner products induce positive definite functions

We reframe the time dependence of the operators as a map on $\mathcal{L}(V)$. Note that the time argument is an element of the group of real numbers \mathbb{R} in the continuous case. When time is discretized (e.g. due to a numerical sampling on an equidistant time grid), it is indexed by an element the group of integers \mathbb{Z} ; we will generically use \mathcal{G} to refer to the group. The time evolution of the operators in the Heisenberg picture is a map ϕ_t that acts on elements of $\mathcal{L}(V)$. That is, for an operator $A(t') \in \mathcal{L}(V)$ and a time argument $t \in \mathbb{R}$,

$$\phi_t : \mathcal{L}(V) \rightarrow \mathcal{L}(V) \quad (16)$$

$$\phi_t A(t') = A(t+t') \quad (17)$$

It is straightforward to show that ϕ_t preserves that group structure of the time argument: $\phi_t \phi_{t'} = \phi_{t+t'}$. Thus, it is a representation of \mathcal{G} . Moreover, for the inner product in Eq. 2, this map is unitary. This can be seen from the relations

$$G_{AB}(t-t') = \langle A(t), B(t') \rangle = \langle \phi_t A, \phi_{t'} B \rangle \quad (18)$$

$$= \langle \phi_{t-t'} A, B \rangle = \langle A, \phi_{t-t'} B \rangle \quad (19)$$

which follow from the cyclicity of the trace. Combining these two points, and because ϕ is a unitary representation of \mathcal{G} , we can show the following theorem.

Theorem 1. *Consider a correlation function of two operators on Fock space $\langle A(t_i), A(t_j) \rangle$. This correlation function is a positive definite function.*

Proof. For a positive definite function evaluated on an arbitrary set of time points t , $f(t_i, t_j)$, the relation

$$\sum_{i,j} f(t_i, t_j) \lambda_i^* \lambda_j \geq 0 \quad (20)$$

holds for any complex vector λ . Expanding out the definition of $\langle A(t_i), A(t_j) \rangle$, it is straightforward to show that

$$\langle A(t_i), A(t_j) \rangle = \text{Tr} \left[\rho \left(\sum_i \lambda_i \phi_i(A) \right)^\dagger \left(\sum_j \lambda_j \phi_j(A) \right) \right], \quad (21)$$

which is the inner product of an element of $\mathcal{L}(V)$ with itself and thus must be ≥ 0 . \square

Thus, $G_{AA}(t - t')$ is a positive definite function.

Connection to Reproducing Kernel Hilbert Spaces

Inner products induce reproducing kernel Hilbert spaces. Given a Hilbert space \mathcal{L} with inner product $\langle \cdot, \cdot \rangle$, the function $K(x, y) = \langle x, y \rangle$ is a kernel function and determines a corresponding reproducing kernel Hilbert space [52] on the space of functions $\mathbb{R} \rightarrow \mathbb{C}$. Reproducing kernel Hilbert spaces form an important tool in statistics and machine learning, with connections to interpolation and approximation theory. This connection will be further examined in a follow-up paper.